mechanism was still unrevealed. We demonstrate a new, conserved actin binding region, called activation loop. It is located at the relay region which swings the lever of myosin upon the powerstroke. We prove that activation loop interacts with the N-terminal segment of actin. We found that this interaction specifically activates myosin ATPase. Biochemical (steady state and transient kinetic fluorescent measurements) and *in vivo* experiments using transgenic *C. elegans* strains proved that activation loop is responsible for force production but not essential for motility *per se*. We conclude that actin binding to activation loop directly accelerates the lever movement. This process increases the ratio of working myosin heads and produce effective muscle contraction.

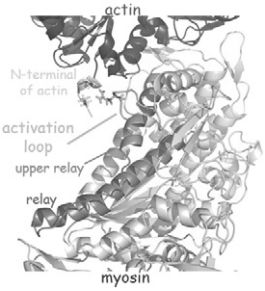

706-Pos Board B506

Interaction of a Novel Fluorescent Non-Nucleotide ATP Analogue with ATP-Driven Molecular Motors

Keiko Tanaka, Taro Kimura, Shinsaku Maruta.

Fluorescent nucleotide analogues are essential for analysis of nucleotide-binding proteins. Most of fluorescent-labeled ATP analogues are ribose-modified. However, they are known to be 2' and 3' isomers mixture. Often these isomers show different properties each other. To avoid isomers, we designed and synthesized non-nucleotide fluorescent ATP-analogue, *N*-methylanthraniloyl amino ethyl triphosphate (MANTTP) which similar structure to the non-nucleotide ATP analogue 2-[(4-azido-2-nitrophenyl) amino] ethyl triphosphate (NANTP). It is known that NANTP are good substrate for skeletal myosin and induces actin gliding in vitro motility assay. Excitation and emission maximums in the fluorescence spectrum MANTTP were 330nm and 430nm, respectively. MANTTP was hydrolyzed by conventional kinesin and skeletal myosin, and induced dissociation of acto-myosin. The MANTTPase of myosin and kinesin were significantly activated by actin and microtubule, respectively. The ADP form of MANTTP showed the formation of skeletal muscle myosin-MANTDP-BeFn complex which mimic the transient state in ATPase cycle and this complex detaches from actin filament. K_{SV} of MANTDP-S-1-phosphate analogue complex showed significantly smaller value than that of free MANTTP. The results suggested that the fluorophore moiety of MANTDP in the complex is buried deeply in the ATP binding site. The fluorescent intensity of MANTTP itself does not change on binding to myosin ATP binding site, however, MANTTP showed significant FRET between intrinsic tryptophan residue of skeletal muscle myosin and MANTTP. The binding of MANTTP to myosin can be observed as fluorescence increase on the stopped flow system. The second-order rate constant for MANTTP first binding to myosin is $0.15\times10^{-6}M^{-1}s^{-1}$. It was shown that the novel fluorescent ATP analogue is applicable to the kinetic studies on ATPases.

Electron and Proton Transfer

707-Pos Board B507

Proton Conduction via Water Wire in the Hv1 Proton Channel

Eric V. Schow, J. Alfredo Freites, Stephen H. White, Francesco Tombola, Douglas J. Tobias.

The voltage-gated proton (Hv1) channel (2006, Science 312: 589; 2006, Nature 440: 1213) is homologous to the voltage-sensing domain (VSD) of voltage-gated ion channels, but unlike ion channels, Hv1 lacks a central pore domain. In Hv1, which forms a dimer, but also functions as a monomer, the VSD serves dual functions: it gates the proton current and also acts as the proton conduction pathway (2008, Neuron 58: 546; 2008, PNAS 105: 9111). In order to understand the proton conduction mechanism in Hv1, we have performed all-atom simulations of Hv1 and its mutants in a lipid bilayer in excess water to an aggregate trajectory length that exceeds 1 μs. To generate our Hv1 structural model, we used the VSD structure of the Kv1.2 paddle-chimera channel (2007, Nature 450: 376) as a template. Because the Hv1 S4 helix contains only three of the four highly conserved arginines (R1-R4) that are known to confer voltage sensitivity in VSDs of Kv channels, we generated two initial model configurations; one where the Hv1 S4 arginines were aligned to R1-R3 of the Kv VSD structure, and a second one where they were aligned to R2-R4. In both models, we observe a water wire that extends through the membrane, and is single file over a stretch of 8Å. In contrast, in a control simulation of the Kv chimera VSD, no waters are observed in the corresponding region. A network of charged residues that includes the S4 arginines as well as several acidic residues coordinates the Hv1 water wire. The presence of multiple basic and acidic residues in the region central to the water wire may explain the robustness of proton conduction in the presence of a variety of mutations (2010, NSMB 17: 869).

708-Pos Board B508

Bovine Cytochrome Oxidase Structures Enable Molecular Oxygen Reduction without Formation of Active Oxygen Species, Providing a Proton Pumping Gate

Shinya Yoshikawa.

The O_2 reduction site of cytochrome c oxidase (CcO), comprising iron (Fe_{a3}) and copper (Cu_B) ions, is probed by X-ray structural analyses of CO, NO and CN^- derivatives to investigate the mechanism of the complete reduction of O_2. Formation of the $Fe_{a3}{}^{2+}$-CN^- derivative contributes to the trigonal planar coordination of $Cu_B{}^{1+}$ and displaces one of its three coordinated imidazole groups while a water molecule becomes hydrogen-bonded to both the CN^- ligand and the hydroxyl group of Tyr244. When O_2 is bound to $Fe_{a3}{}^{2+}$, it is negatively polarized (O_2^-), and expected to induce the same structural change induced by CN^-. This allows O_2^- to receive three electron equivalents non-sequentially from $Cu_B{}^{1+}$, $Fe_{a3}{}^{3+}$ and Tyr-OH, providing complete reduction of O_2 with minimization of production of active oxygen species.

The proton pumping pathway of bovine C*c*O comprises a hydrogen bond network and a water channel which extend to the positive and negative side surfaces, respectively. Protons transferred through the water channel are pumped through the hydrogen-bond network electrostatically with positive charge created at the Fe_a center by electron donation to the O_2 reduction site. Binding of CO or NO to $Fe_{a3}{}^{2+}$ induces significant narrowing of a section of the water channel near the hydrogen-bond network junction, which prevents access of water molecules to the network. In a similar manner, O_2 binding to $Fe_{a3}{}^{2+}$ is expected to prevent access of water molecules to the hydrogen-bond network. This blocks proton back-leak from the network and provides an efficient gate for proton pumping.

709-Pos Board B509

Preferred Pathway of Electron Transfer in the Dimeric Cytochrome b_6f Complex: Selective Reduction of One Monomer

S. Saif Hasan, Stanislav Zakharov, William A. Cramer.

The cytochrome b_6f and bc_1 (cyt *bc*) complexes are symmetric dimeric structures that enclose a central cavity that traps lipophilic quinone/ol from the membrane. The function of the dimer in electron transfer between the two hemes, b_p and b_n, is not known. Cross-over between the two hemes b_p was predicted[1] and recently observed.[2,3] although the branching ratio for cross-over is not known. Consideration of inter-heme distances in the photosynthetic bacterial bc_1 complex,[4] and in a range of cytochrome *bc* complexes[5] imply that the intra-monomer pathway (b_p-b_n) is significantly preferred over a pathway involving cross-over between the two hemes b_p. Split circular dichroism spectra in the Soret band of cytochrome *bc* complexes, (node of the CD spectra in the Soret band coincides with the absorbance maximum of hemes) imply that two *b*-hemes interact excitonically.[6] Consideration of inter-heme distances and angular orientations imply that exciton interaction in the Soret absorbance band detected by CD arises between reduced hemes b_p and b_n. Reduction of the b_6f complex by NADPH-ferredoxin in thylakoid membranes,[7] or for cyanobacterial b_6f complex isolated in detergent,[8] accomplishes the reduction of no more than half of the *b* heme in the complex. It is inferred that enzymatic reduction by FNR bound to the complex reduces hemes b_p and b_n in only one monomer of the dimer, perhaps because only one FNR can occupy the *n*-side (stromal) docking site of the dimer. It is inferred that inter-monomer b_p - b_p electron crossover is inefficient in this experiment (Support: NIH GM38323). *References*: [1]Soriano *et al*., 1999; [2]Swierczek *et al*. 2010; [3]Lanciano *et al*. 2010; [4]Shinkarev & Wraight 2007; [5]Cramer *et al.* 2010, in preparation; [6]Palmer & Degli-Esposti 1994; [7]Furbacher *et al*. 1989; [8]Yamashita *et al*. 2007.

710-Pos Board B510

Design of Transmembrane Electron Transport Chain within Amphiphilic Protein Maquettes

Bryan A. Fry, Gregory R. Wiedman, Christopher C. Moser, P. Leslie Dutton, Bohdana M. Discher.

Electron transport chains are fundamental to both photosynthesis and oxidative phosphorylation. Protein-based electron transport chains transfer electrons from high-energy donors to lower-energy acceptors and are commonly coupled to the translocation of protons across a membrane, producing a transmembrane electrochemical potential gradient. Electron transfer rates within these chains are governed primarily by the distance between redox centers and by the driving force that originates from the redox mid-point potentials or coupled catalytic reactions. The complexity of natural redox protein structures contrasts the relatively simple rules of cofactor placement that, in principle, govern the electron transfer behavior.

Rather than focusing on the structural details of a specific natural protein, we are designing general protein structural scaffolds (''maquettes'') to accommodate a variety of functions. Here we will present transmembrane electron transfer via AP6, an amphiphilic tetra-helical maquette that binds up to 6 hemes. We demonstrate that AP6 self-assembles with phospholipids into vesicles. Our stop flow experiments confirm that the AP6 maquette significantly increases the electron transfer rates between oxidizing interior and an external redox mediator dye, as shown below.

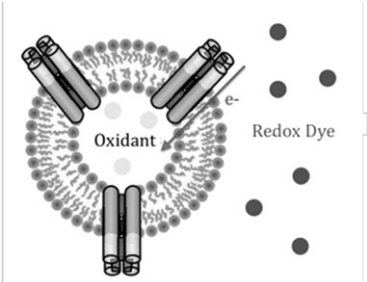

711-Pos Board B511
Expression and Characterization of Cytochrome C6 from Chlamydomonas Reinhardtii using a Designer Gene
Nicole L. Vanderbush, Brian St. Clair, Marylyn Davis, Dan Davis.
Cytochrome c6 is a lumenal redox carrier in oxygenic photosynthesis. We have constructed a synthetic gene, expressed, purified, and coducted an initial characterization for the cytochrome c6 from Chlamydomonas reinhardtii. The synthetic gene was constructed by the removal introns and the substitution of codons for those best suited for expression in E. coli. The gene was incorporated into a pUCF2 plasmid in place of cytochrome f, downstream of the lac operon and a pelA leader sequence. The protein is expressed by a cotransformation in E. coli with the plasmid containing the c6 gene and the PEC86 plasmid, which contains a set of genes for the covalent attachment of the heme to the protein. The spectral characteristics of the protein were determined using a UV-Vis spectrophotometer and include a reduced α peak at 553nm, β peak at 523nm, and a Soret band at 417nm. The midpoint potential at pH 7 was determined by redox titrations and found to be 365 $\pm$ 5mV. Differential scanning calorimeter experiments also reveal that the folding of the wild-type protein is irreversible and that the Tm for the protein is 78°C. Two mutants of the protein , K29I and K57I, were constructed using site-directed mutagenesis. The redox potential of the K57I mutant was found to be 20mV lower than the wild-type protein. The mutants both fold irreversibly like the wild-type but their Tm's are lower at 70°C for the K29I mutant and 71°C for the K57I mutant.

712-Pos Board B512
Tuning the Intramolecular Electron Transfer in 2[4Fe-4S] Ferredoxin: A Molecular Dynamics Study
Ming-Liang Tan, Yan Luo, Toshiko Ichiye.
The 2[4Fe-4S] ferredoxins are found as a subunit of Photosystem I and of the respiratory complex I ''wire'' and as water-soluble proteins in bacteria. They are generally small (6 kDa) pseudosymmetric proteins containing two [4Fe-4S] clusters. The effects of protein and solvent on the intramolecular electron transfer direction and rate are studied. Interestingly, while the charged side chains overwhelmingly favor the reactant state and the rest of the polar groups of the protein only slightly favor the product state, the solvent and counterions overwhelmingly favor the product so that the net driving force slightly favors the product, in agreement with experiment.

713-Pos Board B513
Electrical Transport along Bacterial Nanowires
Tom Yuzvinsky, Moh El-Naggar, Greg Wanger, Kar Man Leung, Gordon Southam, Jun Yang, Woon Ming Lau, Kenneth Nealon, Yuri Gorby.
Bacterial nanowires are extracellular appendages that have been suggested as pathways for electron transport in phylogenetically diverse microorganisms, including dissimilatory metal-reducing bacteria, photosynthetic cyanobacteria, and thermophilic fermentative bacteria. The presence of bacterial nanowires in organisms across the metabolic spectrum challenges our understanding of extracellular electron transfer in microbial communities and has significant biotechnological implications for renewable energy recovery in microbial fuel cells. To date, several biological assays have demonstrated results consistent with electron transport along bacterial nanowires, but our direct knowledge of nanowire conductivity has been limited to local scanning probe measurements across the width of nanowires. We will present electron transport measurements along the length of individually addressed bacterial nanowires derived from electron-acceptor limited chemostat cultures of the dissimilatory metal reducing bacterium Shewanella oneidensis MR-1. We will also discuss the results of transport measurements on intact biofilms and the contribution of nanowires to their overall conductivity.

Membrane Transport

714-Pos Board B514
Computer Simulation of TolC Ground State Dynamics and Spontaneous Binding of the AcrB Docking Domain
Martin Raunest, Nadine Fischer, Christian Kandt.
In Escherichia coli the AcrAB-TolC efflux pump expels a broad range of drugs and other molecules. While AcrB is the engine in this system, the outer membrane protein TolC functions as an efflux duct interacting with numerous inner membrane translocases. TolC occurs in at least two states, one that is impermeable for drugs and one where drug passage is possible. We performed a series of five independent, unbiased 150ns molecular dynamics (MD) simulations of wildtype TolC 1EK9 embedded in a phospholipid/water environment at 0.15M NaCl concentration. One of these runs was extended to 300ns in three independent copies. Whereas TolC remains closed between a 1st bottleneck region outlined by Asp-374 &371, we observe opening and closing motions in a 2nd bottleneck region near Gly-365. While previous studies reported a frequent binding of potassium ions stabilizing a closed TolC conformation in the bottleneck II region, we observe a frequent passage of sodium ions. However, in one simulation a consecutive binding of two sodium ions occurs between Gly-365 and Asp-374 leading to a closed TolC conformation at the AcrB interface, which was stable for more than 175ns. To gain insight into TolC-AcrB interaction, we performed five independent unbiased 150ns MD simulations of TolC and the AcrB docking domain (AcrB_dd). Initially placed 1 nm away from TolC and identically oriented as in the AcrAB-TolC Symmons docking structure, AcrB_dd spontaneously docks to TolC in one run. Extending this simulation to one micro second, we find an TolC-AcrB_dd docking interface characterized by a larger contact area and a slight asymmetry not present in the Symmons model. At the same time TolC opens in the bottleneck II region. All simulations were performed using GROMACS 4.0.3 and the G53a6-GROMOS96 force field.

715-Pos Board B515
Computational and Experimental Studies of Substrate Binding, Conformational Change and Importance of the Trimeric State in the Glycine Betaine Transporter BetP
Kamil Khafizov, Camilo Perez, Ching-Ju Tsai, Christine Ziegler, Lucy R. Forrest.
The glycine betaine/sodium symporter BetP responds to changes in external osmolality by regulation of its transport activity. A recent X-ray structure of BetP confirms that it is a homotrimer and in this structure each protomer adopts an identical conformation, in which the pathway is occluded from both sides. Despite the availability of a wealth of experimental data for BetP, the structures of the alternate states (e.g., open to the outside of the cell), molecular mechanisms of substrate and Na+ binding and transport, as well as the functional implications of the trimeric state remain poorly understood. To address these questions, we carried out computational studies using a range of techniques to derive hypotheses that were then tested experimentally. First, to identify structural features of the alternate states, we developed a procedure for flexible fitting of the X-ray structure of BetP into a lower-resolution cryo-EM map of BetP in a more native lipid environment, in which the three protomers have different conformations. These results suggest that: (i) the protomers adopt distinct conformational states relevant to the transport cycle; and (ii) there is conformational coupling between the protomers. Second, we performed all-atom molecular dynamics simulations and in silico alanine scanning of BetP trimers in order to identify interface residues crucial for maintaining the trimeric state. Mutations of these residues to alanine were introduced experimentally revealing that the isolated monomers are functional, and that the trimeric state is important for the regulation and higher activity of the protein. Finally, using molecular modeling and biochemical experiments we identified two Na+ binding sites in BetP that could not be resolved in the 3.35 Å resolution X-ray structure.

716-Pos Board B516
Mathematical Model of the Regulatory Cell Volume Decrease
Aleksandr V. Ilyaskin, Galina Baturina, Evgeniy I. Solenov, Aleksandr Ershov, Dmitriy Medvedev, Denis Karpov.
Renal collecting duct principal cells perform vasopressin regulated water reabsorption and form the composition of tubular fluid. The osmotic pressure of the extracellular fluid varies significantly. To maintain viability in hypotonic